energies

Article

Assessment and Duration of the Surface Subsidence after the End of Mining Operations

Mateusz Dudek, Anton Sroka, Krzysztof Tajduś, Rafał Misa * and Dawid Mrocheń

Instytut Mechaniki Górotworu PAN, ul. Reymonta 27, 30-059 Kraków, Poland
* Correspondence: misa@imgpan.pl; Tel.: +48-12-637-62-00

Abstract: The change in the European Union's policy related to the energy transformation of Europe and the departure from fossil energy resources may contribute to the accelerated closure of many coal mines. Therefore, it is necessary to solve the problem of surface subsidence after the end of underground mining and the related suitability of post-mining areas for the re-use of the so-called problem of the reclamation of post-mining areas. In the case of areas suitable for re-use, it is necessary to determine the value of the final subsidence. It is also important to specify the time after which mining influences will no longer have a significant impact on the surface infrastructure and the environment. Analyses of the observed subsidence after the end of the mining operation indicate that this process may last from several months to several dozens or even several hundreds of years. It depends on the individual characteristics of the mining area, including the depth of exploitation, mining system, the behavior of the surrounding rock mass, etc. The article presents an in-depth analysis of residual subsidence and its duration using the proprietary forecasting method and the Gauss–Markov algorithm based on the example of the German Lohberg mine (Ruhr District), whose mining activity was completed in January 2006.

Keywords: residual subsidence; forecasting; land surface deformation; Gauss–Markov algorithm; mining damages

Citation: Dudek, M.; Sroka, A.; Tajduś, K.; Misa, R.; Mrocheń, D. Assessment and Duration of the Surface Subsidence after the End of Mining Operations. *Energies* **2022**, *15*, 8711. https://doi.org/10.3390/en15228711

Academic Editor: Piotr Małkowski

Received: 21 October 2022
Accepted: 17 November 2022
Published: 19 November 2022

1. Introduction

The increase in social sensitivity to environmental aspects observed in recent years, along with the global tendency to increase the costs of hard coal mining and, at the same time, the increasing cost of the liquidation of underground deposits, led the authorities of many countries to decide to close some underground mines. This situation especially occurs in Europe, where mining has been conducted for hundreds of years. The process of the liquidation of underground mines is carried out using various methods, and they depend on mining and geological conditions, mining technology, costs, the nature of the deposit, etc., described in the works [1–3]. The authors of these articles also identified the potential environmental hazards that may occur during the mine closure process [4,5]. However, as reality shows, the process of the liquidation of mines, e.g., by flooding, due to its complicated legal and technical situation, often begins several years after the end of underground mining [6–9]. During this period, the rock mass is subject to constant movements related to both the influence of technical works on the surrounding rock mass (e.g., mine drainage) and also the successive reconsolidation of rocks in the caved zone located directly above the exploited seam and the associated compaction of this zone progressing over time. The compaction period may last for many years and depends on the degree of rock mass disturbance, its quality, the exploitation systems used, the depth of works, tectonics, water inflow, the mechanical parameters of rock layers, the time of mining works, and many other factors. The land surface movements caused by the above factors, recorded after the end of the exploitation process, are called residual subsidence.

State of the Art

In world literature, a few researchers have dealt with the problem of assessing the occurrence of this type of subsidence, focusing mainly on monitoring and describing the phenomenon [10–13] rather than modeling [14]. This was due to the fact that scientists focus on the problem of subsidence in the initial and main phases (lasting up to about 1 year after the end of mining operations), which occur during the mining operation. This subsidence accounts for approx. 90% of all subsidence of the land surface, with only approx. 10% attributed to residual subsidence. For this reason, the problem of residual subsidence was ignored from the point of view of operational safety and potential mining damage. However, the aforementioned change in the energy policy and the intensification of the mine closure process led to an increased interest in the problem of residual subsidence, both among scientists and the mining industry.

The first studies on calculating the development of the subsidence trough in time come from the 1950s. In 1953, Knothe [15] formulated a time function to describe the course of the subsidence trough. The reason for scientific studies in this area was in situ observations and experiments saying that the values of the maximum deformation indices characteristic for the transitional (unsteady, dynamic) troughs are significantly lower than those for the final (fixed, static) troughs. The basis of the solution given by Knothe was the assumption that the speed of the point at time t is proportional to the difference between the final subsidence s_e, which the point may undergo as a result of selecting a certain part of the seam, and the size of the point subsidence $s(t)$ at any time (Formula (1)):

$$\dot{s}(t) = \frac{\partial s(t)}{\partial t} = c[s_e - s(t)] \tag{1}$$

where:

c—subsidence velocity coefficient, the value of which depends on the properties of the rock mass in the area of exploitation.

Solving Equation (1), taking into account the initial condition $s\ (t = 0) = 0$, can be achieved:

$$s(t) = s_e[1 - \exp(-ct)] = s_e \cdot f(t) \tag{2}$$

where:

$f(t) = 1 - \exp(-ct)$—the so-called function of time.

The assumption that the value of final subsidence s_e during the mining operation is constant does not correspond to reality. This value is variable during exploitation and takes a constant value only after its completion or when the considered point is beyond the range of the mining exploitation. It follows that the time function $f(t)$ describes only the part of the subsidence process that takes place after the end of the mining.

Assuming that the value $s_e(t)$ is a function of time leads to the differential Equation (1). The solution to this equation, taking into account the initial condition $s(t = 0) = 0$, is Equation (3):

$$s(t) = s_e(t) - \exp(-ct) \int_0^t \dot{s}_e(\lambda) \exp(c\lambda) d\lambda \tag{3}$$

where:

$\dot{s}_e(t) = \frac{\partial s_e(t)}{\partial t}$, andthe value $s_e(t)$ indirectly describes the history of mining operations up to the moment t [16]

The solution of the course of subsidence in time presented above in the following years was modified many times by many scientists from around the world. A two-parameter model of the time function was presented by Schober and Sroka [17] describing the process of the subsidence caused by the convergence of salt caverns for the storage of fluidized energy medium (4):

$$f(t) = 1 + \frac{\xi}{c - \xi} \exp(-ct) - \frac{c}{c - \xi} \exp(-\xi t) \tag{4}$$

where:

c—the time factor for the process of passing through the rock mass, and

ξ—the relative velocity of cavern volume convergence (salt creep velocity) depending on the course of its use, depth of location, and the mechanical properties of the salt rock.

In 2017, Chen et al. [18] noticed that the time function c presented by Knothe can be presented as a power function in the form:

$$c(t) = m \cdot t^{k-1}, \tag{5}$$

where t and k are dimensionless parameters of the model. Based on the Equation (4), Chi and the team [19] proposed adding a new coefficient $\left(\frac{H}{h_s}\right)^n$, where H is the depth of exploitation, h_s is the thickness of the unconsolidated layer, and n is the dimensionless parameter of the model. According to the authors, the parameters m, k, and n are closely related to the geological conditions in the area of exploitation and should be optimized using modern optimization methods such as genetic algorithms, particle swarm optimization, etc., according to the function $[w_i - w(t, m, k, n)]^2 = min$.

Chang and Wang [20] established a subsection prediction model by analyzing the two-stage subsidence process of surface points. They expressed the second half of the subsection Knothe function subsidence rate formula through the subsidence rate formula of the Knothe function. Deng et al. [21] analyzed the subsidence velocity of any point on the surface during mining and pointed out that "the surface subsidence velocity curve can be approximately regarded as a symmetrical distribution". This formulation can symmetrically represent the first half of the subsidence velocity formula of the piecewise Knothe function:

$$\begin{cases} V_1(t) = \frac{1}{2} C W_{max} e^{-C(\tau - t)}, \ 0 < t < \tau \\ V_2(t) = \frac{1}{2} C W_{max} e^{-C(t - \tau)}, \ \tau < t \end{cases} \tag{6}$$

The improved Knothe subsidence influence function model [22] (Model II) can be deduced:

$$\begin{cases} W_1(t) = \frac{1}{2} W_{max} \left[e^{-C(\tau - t)} - e^{-C\tau} \right], \ 0 < t < \tau \\ W_2(t) = \frac{1}{2} W_{max} \left[2 - e^{-C(\tau - t)} - e^{-C\tau} \right], \ \tau < t \end{cases} \tag{7}$$

In Equation (6), it is assumed that t (the time associated with the maximum subsidence) is half of the total duration of subsidence. The corresponding value of subsidence at its maximum speed is half of the amount of the maximum subsidence, and the time influence coefficient, C, has a fixed value.

Lian et al. [23] reviewed and extended an existing classical prediction model of the dynamic subsidence [24] and proposed potential new research avenues offered by Cellular Automata (CA) models based on the probabilistic evolution rules.

Hu et al. [25], based on the stochastic medium theory micro-model and the hypothesis of Knothe dynamic subsidence, proposed new approach to the dynamic prediction model for the entire mining process. Essentially, the authors establish the new dynamic subsidence prediction model using the standard Knothe model and stochastic medium theory.

In turn, Han et al. [26] established a composite function model based on an inverted analysis of measured data. The results showed that the composite function model could describe the whole subsidence and agreed well with the measured data.

Zhang et al. [27] adopted the probability integral method, dual-medium method, and least square method, combined with field-measured data, to determine C and the model order n used in proposed Equation (8), where C is a time influence parameter of the improved Knothe time function model, with this parameter expressed in the unit $\frac{1}{year}$. Authors made a new assumption in the improved Knothe time function model: the $n - th$ surface subsidence derivative $\frac{d^n W(t)}{d^n t}$ is proportional to the n-th power of the difference between the final surface subsidence W_0 and the dynamic subsidence $W(t)$ at time t.

$$\frac{d^n W(t)}{d^n t} = C[W_0 - W(t)]^n \quad (8)$$

A similar approach has been proposed by Cheng at al. [28]. An improved Knothe time function model was recommended and established via analogical reasoning from a phenomenological perspective based on an inverse 'Hohai creep model' function in accordance with the antisymmetric relationship between the unstable creep curve and surface dynamic subsidence curve. The authors proposed the use of an improved Knothe model expression as follows (Formula (9)):

$$\frac{dW(t)}{dt} = Cnt^{n-1}[W_0 - W(t)] \quad (9)$$

where C is a time influence parameter of the improved model and n is the model order.

The result of the error analysis shows that the average relative standard deviation of the improved model was only 4.9%, which is lower than the 23.1% of the standard Knothe model. The improved model can describe the actual process of surface subsidence containing only two model parameters C and n, which is convenient for practical engineering application.

2. Materials and Methods

2.1. Methodology of Residual Subsidence Calculation

The basis of the presented innovative solution was the use of the Gauss–Markov algorithm for the so-called indirect (or intermediary) observations to determine the prognostic value of the future subsidence of the area. This algorithm basically requires knowledge of two basic elements (Figure 1):

- A functional model that connects the directly observed values (here: subsidence after the end of the mining operation) with the unknowns (here: time coefficient and final subsidence value);
- A stochastic model of the observed values.

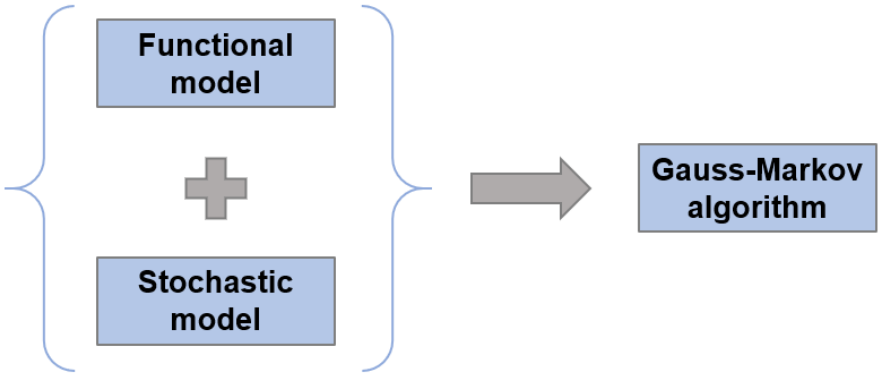

Figure 1. Methodology used for estimating long-term impacts of mining operations (residual subsidence and their duration) using the Gauss–Markov algorithm.

The Gauss–Markov algorithm allows for the identification of the most probable values of the parameters of the functional model on the basis of in situ subsidence measurements and then, for their further prediction, for $t > t_n$.

2.2. Functional Model

The authors, based on many years of experience in forecasting and modeling land surface deformation caused by underground mining, decided to use a functional model based on the Knothe method [24]. The value of $s_e(t)$ presented in Formula (3) indirectly describes the course of the history of mining up to the moment t [16]. Assuming that

mining is finally terminated at time $t = T$, the course of subsidence for time $t \geq T$ will be described by the following formula:

$$s(t \geq T) = s_e(T) + [s_e(T) - s(T)][1 - \exp(-c(t - T))] \quad (10)$$

where:

$s(T)$—the subsidence at the end of mining operations;

$s_e(T)$—the characteristic of the mining operation carried out up to the time t of the final settlement value.

A detailed explanation of Formula (10) is presented in Figure 2.

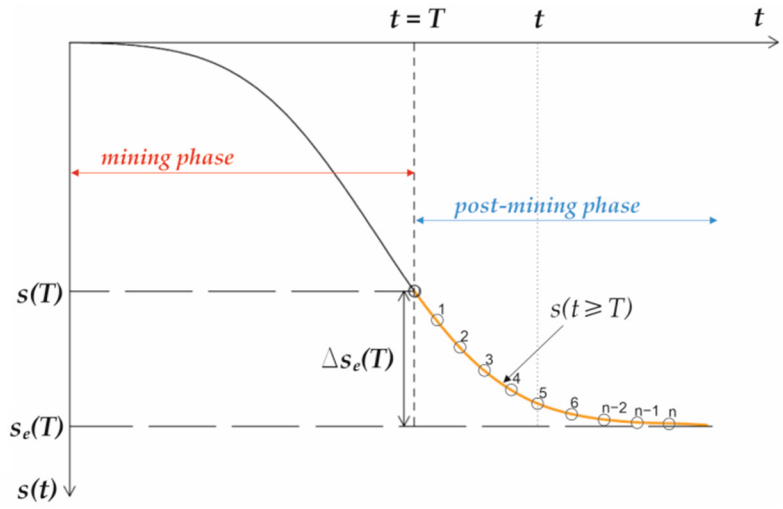

Figure 2. The course of subsidence after the end of mining exploitation—illustration for Formula (10).

In most cases, there are no results of measurements taken at the end of mining operations. The starting points for the analysis of the course of subsidence is the first subsidence s_1 measured after the end of mining operations in time t_1. Then, Formula (10) takes the following form:

$$s(t \geq t_1) = s_e + [s_e - s_1][1 - \exp(-c(t - t_1))] \quad (11)$$

where:

$$s_e = s_e\ (T)$$

2.3. The Stochastic Model

In the case where the number of measurements is $n > 3$, the evaluation of the parameters of the method specified in the functional model can be performed using the Gauss–Markov algorithm [29]. The Gauss–Markov algorithm is the basis of the presented solution for the so-called indirect (or intermediary) observations. As mentioned earlier, this algorithm requires knowledge of two basic elements, which are the functional model (described in the previous chapter) and the stochastic model, which always informs about the accuracy of the performed subsidence observations. The determination of the value of the unknowns proceeds in the Gauss–Markov equalization algorithm according to the principle:

$$\underline{V}^T \underline{P} \underline{V} \rightarrow min! \quad (12)$$

where:

$\underline{V}$—the vector of corrections to the measured subsidence values;

$\underline{P}$—the weight matrix of individual observation cycles.

If the accuracy of the measurements of subsidence in each observation cycles is equal, then the assessment of unknowns c, s_1, and s_e is carried out according to the principle:

$$\underline{V}^T \underline{V} \rightarrow min! \quad (13)$$

Principle (12) and (13) are equivalent to determining the value of the time coefficient, the value of subsidence at the time of the end of mining activity, and the final subsidence leading to the best possible adjustment of the values of the measured subsidence by means of a functional model.

There is a stochastic relationship between the adjusted values of the measured subsidence and the most probable values of the unknowns (here: the time coefficient $\hat{c}$, subsidence at the end of mining operations $\hat{s}_1$, and the final subsidence value $\hat{s}_e$):

$$\underline{\hat{S}} = \underline{S} + \underline{v} = \underline{\varphi}(\underline{\hat{B}}) \tag{14}$$

This relationship leads to corrections:

$$\underline{v} = \underline{\varphi}(\underline{\hat{B}}) - \underline{S} = \underline{\varphi}\left(\underline{\hat{X}}\right) - \underline{S} \tag{15}$$

where:

$\underline{S}$—the vector of observed subsidence values;

$\underline{\hat{S}}$—the vector of aligned (fitted) subsidence values;

φ—the functional model;

$\underline{\hat{B}}$—the vector of the values of the parameters of the subsidence model sought;

$\underline{\hat{X}}$—the vector of unknowns;

$\underline{v}$—the vector of corrections.

If the relation (15) is non-linear, linearization should be performed by expanding the Taylor series. It is necessary for the linearization to provide approximate values of unknowns, i.e., approximate values of the parameters of the subsidence model $\underline{B}^0$. These parameters can be estimated using, inter alia, the three or four-point method [30].

After linearization, the correction equation takes the form:

$$\underline{v} = \left(\frac{\partial \underline{\varphi}(\underline{X})}{\partial \underline{X}}\right)_0 \cdot \underline{\hat{x}} + \underline{\varphi}\left(\underline{X}^0\right) - \underline{S} \tag{16}$$

where:

$\underline{\hat{x}} = \underline{\hat{X}} - \underline{X}^0$—the vector of reduced values of unknowns;

$\underline{X}^0$—the vector of approximate values of unknowns.

In the matrix description, the correction Equation (15) can be written in the form (17):

$$\underline{v} = \underline{A}\,\hat{x} - \underline{l}\hat{c}_i \tag{17}$$

where:

$\underline{A}$—the matrix of coefficients of correction equations;

$\underline{l} = \underline{S} - \underline{S}^0$.

According to the principle of the Gauss–Markov algorithm, the solution to the system of the obtained correction equations is:

$$\hat{x} = \left(\underline{A}^T \underline{P}\, \underline{A}\right)^{-1} \cdot \underline{A}^T P\, \Delta \underline{l} \tag{18}$$

and, finally:

$$\hat{X} = \underline{X}^0 + \hat{x} \tag{19}$$

The accuracy of the determined unknowns is determined by calculating the variance–covariance matrix $\underline{M}$ of the determined values of the unknowns:

$$\underline{M} = s_0^2 \cdot \underline{Q} \tag{20}$$

where:

$$s_0 = \sqrt{\frac{\sum_1^n (\hat{s}_i - s_i)^2}{n-u}};\ \underline{Q} = \left(\underline{A}^T \underline{P}\, \underline{A}\right)^{-1};$$

s_0—the total standard deviation of the performed measurements and the functional model;

$\hat{s}_i$—the subsidence after correction;

s_i—the measured subsidence;

n—the number of observations;

u—the number of unknowns ($u = 3$).

3. Results

In 2017–2018, studies were conducted on the course of subsidence after the end of hard coal mining exploitation in the Ruhr Basin. The research work concerned the West Neu, Lippe, Ost, Auguste Victoria, Walsum, and Lohberg mines (Figure 3).

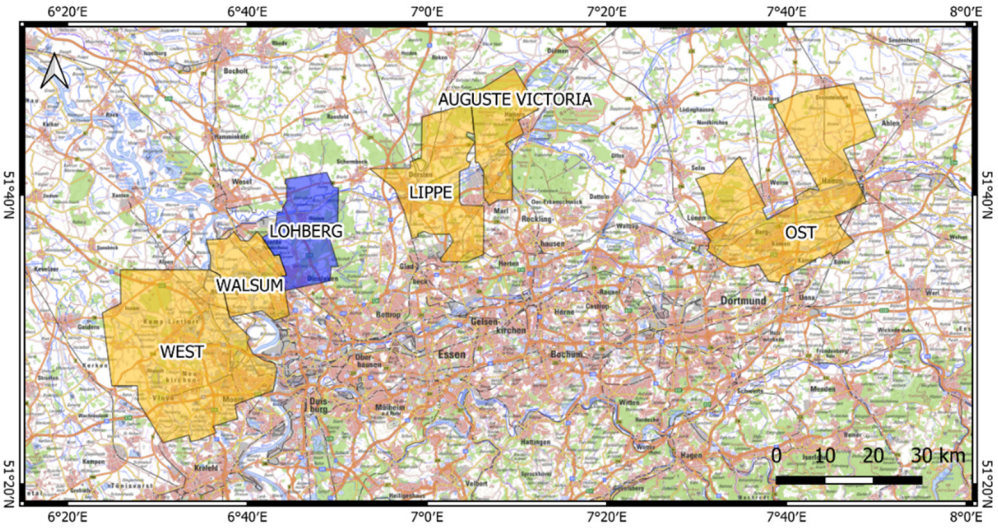

Figure 3. Map with marked regions under analysis in order to estimate residual subsidence and their duration.

These studies concerned the determination of the final subsidence value of selected observation points and the estimation of the time of the completion of the subsidence process. The basis of the conducted analyses and research was the cyclical leveling measurements carried out by the Measurement Office of the State of North Rhine-Westphalia, every 2 or 6 years. On the basis of the performed measurements and the use of the developed methodology based on the Gauss–Markov algorithm, calculations of potential future land surface subsidence were carried out. The results of the forecast calculations are presented for the example of the Lohberg mine belonging to the RAG AG concern.

The geological conditions in the study area (Lohberg mine) are characterized by quaternary and tertiary deposits near the surface. Below these, the rock mass range is built up by strata of the Cretaceous and the Triassic. In the northwest of the study area, these overlay the layers of the Zechstein. Through the mining of hard coal, rocks containing seams from the Upper Carboniferous have been exposed and their storage conditions have been examined. The Upper Carboniferous consist of layers of Westphalia A (Bochum layers) and Westphalia B (Horst and Essen layers), with a total thickness of approx. 650 m.

The Lohberg mine ended its mining operations in January 2006. Hard coal mining in the Lohberg mine was mostly carried out using the longwall panel method. Currently (in the second half of 2022), the mine is in the initial stage of flooding according to the plan developed by the mining company RAG AG. Measurements of the height of the land surface observation points were carried out with the use of precision leveling with an accuracy greater than ±1.0 mm, which leads to an accuracy of the measured subsidence (differences in the height of the point at different times) of ±1.0 mm. Figure 4 shows the Lohberg mine area with the locations of the measuring points. For the proper analysis, six

points were selected, in which, the mining activity was completed in 2006. These are the measurement points: 121, 104, 170, 199, 209, and 212.

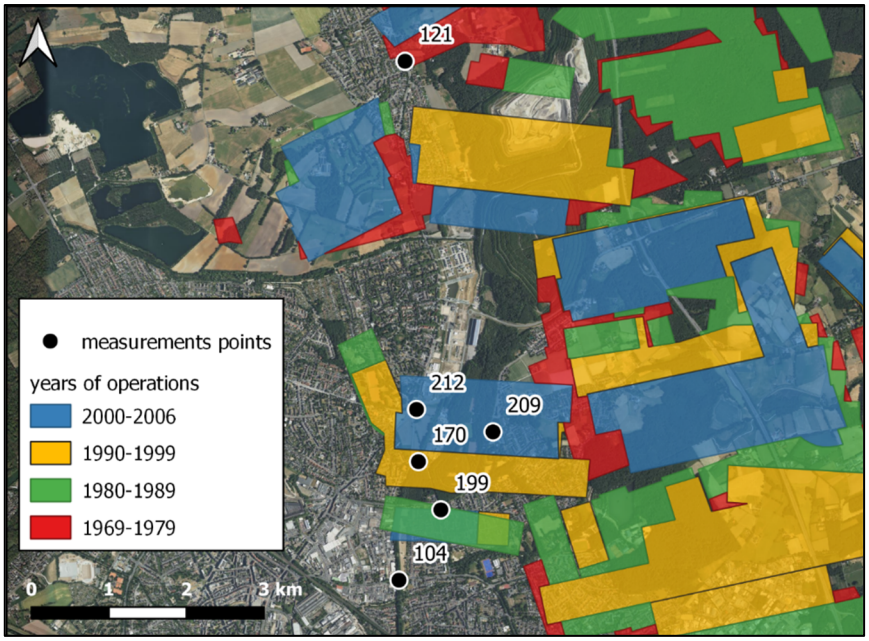

Figure 4. Map of the Lohberg mine area with the location of the measurement points selected for the analysis and exploitation carried out.

A prognostic analysis was performed in order to determine the final value of the subsidence of the measurement point and to determine the necessary time of the observation of the vertical displacement. The analysis was carried out using the Gauss–Markov algorithm. Table 1 shows the values of land surface subsidence at all analyzed measurement points in the period from 2008 to 2018.

Table 1. Values of measured subsidence s_{meas} of measuring points in two-year intervals until 2018.

Year	Point Number					
	121	**104**	**170**	**199**	**209**	**212**
	s_{meas} **[mm]**					
2008	774	773	6285	1247	1314	635
2010	781	785	6310	1267	1348	667
2012	790	793	6331	1281	1371	693
2014	797	800	6352	1295	1396	718
2016	800	800	6362	1300	1410	735
2018	807	808	6380	1313	1427	754

To estimate the value of the residual subsidence, it is necessary to know the parameters of the functional model, which, in the analyzed problem, is the Knothe time function (1). For the calculations carried out in accordance with the Gauss–Markov algorithm, the following values of the time coefficient and the final subsidence in the analyzed point 121 were obtained:

$$\hat{s}_1 = 773.66\ [\text{mm}],\ \hat{c} = 0.0659\ \left[\text{year}^{-1}\right],\ \hat{s}_e = 841.93\ [\text{mm}]$$

$$s_{s_1} = 1.25\ [\text{mm}],\ s_c = 0.0342\ \left[\text{year}^{-1}\right],\ s_{se} = 25.78[\text{mm}]$$

where:

s_{s_1}, s_c, s_{se}—standard deviations of the identified model parameters.

Further analyses were carried out analogously for the remaining measuring points in the area of the Lohberg mine. Table 2 contains the initial and final parameters obtained from simulations with the Gauss–Markov algorithm. On the other hand, Table 3 illustrates the obtained vertical displacements from the simulation s_{calc} compared to the surface measurements s_{meas} until 2018. The course of total subsidence for all analyzed points and the forecast of residual movements after the end of the mining operation are shown in Figures 5–10.

Table 2. Initial (calculated using 3- or 4-point method [30]) and final parameters using the Gauss–Markov equalization algorithm.

Point Number		Calculated Subsidence [mm]					
		121	**104**	**170**	**199**	**209**	**212**
Initial	s_1^0	774.00	773.00	6285.00	1247.00	1314.00	635.00
	s_e^0	813.00	832.10	6444.80	1355.30	1540.70	808.20
	c_0	0.1437	0.0957	0.0933	0.0953	0.0813	0.1133
Final	$\hat{s}_1$	773.66	772.87	6285.07	1247.48	1313.97	634.97
	$\hat{s}_e$	841.93	814.40	6458.26	1344.08	1491.16	854.08
	$\hat{c}$	0.0659	0.1640	0.0777	0.1060	0.1001	0.0777

Table 3. Results of the subsidence obtained using the Gauss–Markov equalization algorithm in analyzed point.

Year	Subsidence at Measuring Points [mm]					
	121		104		170	
	s_{meas}	s_{calc}	s_{meas}	s_{calc}	s_{meas}	s_{calc}
2008	774.00	773.66	773.00	772.87	6285.00	6285.07
2010	781.00	782.06	785.00	784.363	6310.00	6309.69
2012	790.00	789.41	793.00	792.676	6331.00	6330.73
2014	797.00	795.85	800.00	798.688	6352.00	6348.72
2016	800.00	801.49	800.00	803.036	6362.00	6364.10
2018	807.00	806.43	808.00	806.181	6380.00	6377.25
Year	Subsidence at Measuring Points [mm]					
	199		209		212	
	s_{meas}	s_{calc}	s_{meas}	s_{calc}	s_{meas}	s_{calc}
2008	1247.00	1247.48	1314.00	1313.97	635.00	634.97
2010	1267.00	1265.93	1348.00	1346.12	667.00	666.51
2012	1281.00	1280.86	1371.00	1372.43	693.00	693.50
2014	1295.00	1292.94	1396.00	1393.97	718.00	716.62
2016	1300.00	1302.71	1410.00	1411.61	735.00	736.40
2018	1313.00	1310.61	1427.00	1426.04	754.00	753.34

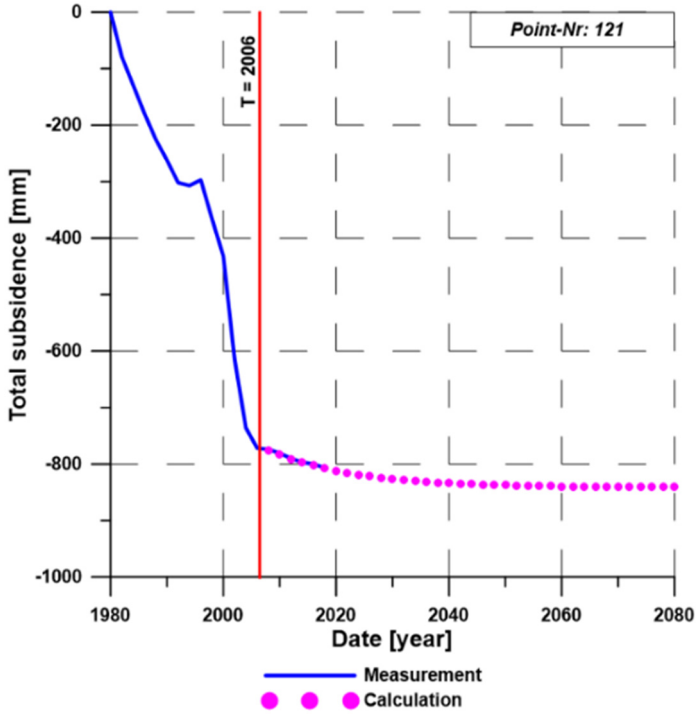

Figure 5. The course of subsidence until 2018 and the prediction of residual subsidence for the point no. 121.

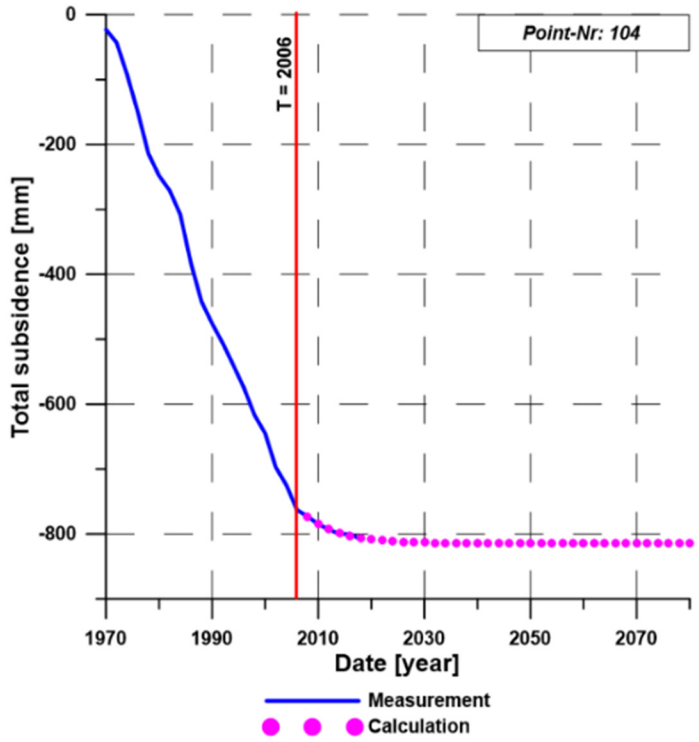

Figure 6. The course of subsidence until 2018 and the prediction of residual subsidence for the point no. 104.

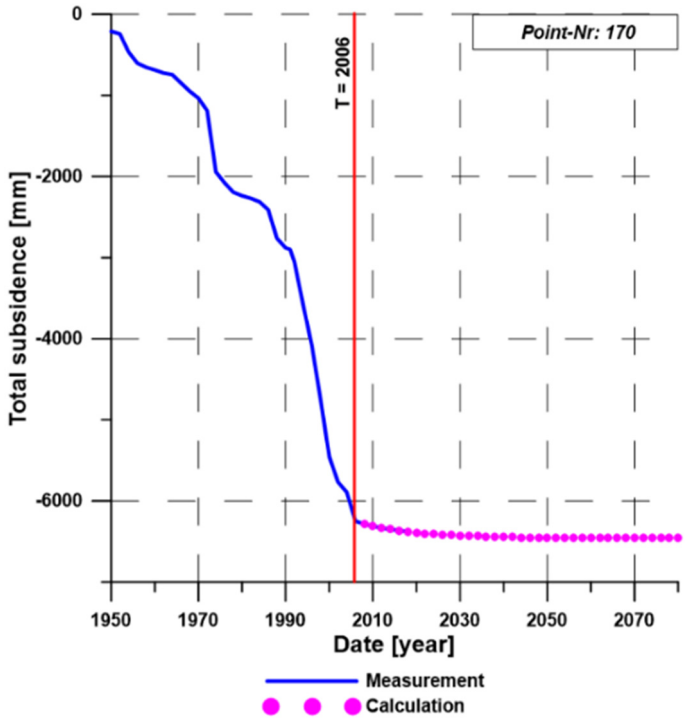

Figure 7. The course of subsidence until 2018 and the prediction of residual subsidence for the point no. 170.

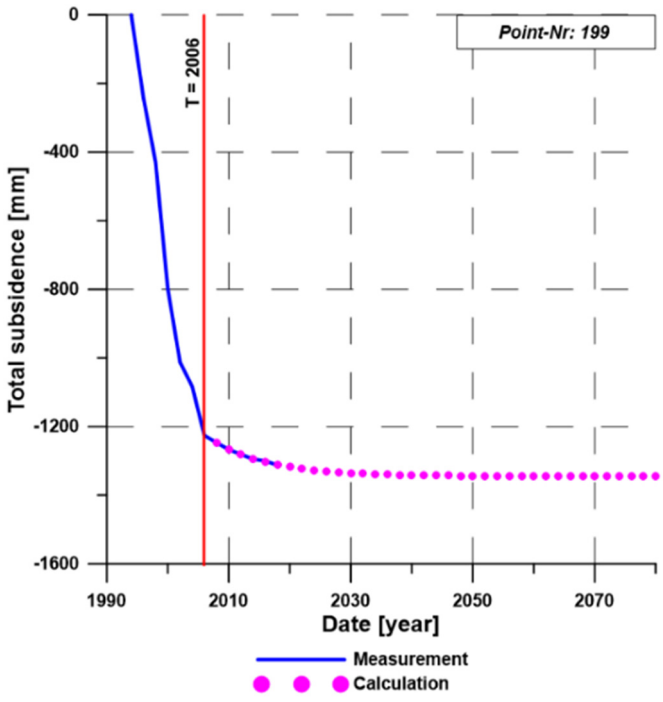

Figure 8. The course of subsidence until 2018 and the prediction of residual subsidence for the point no. 199.

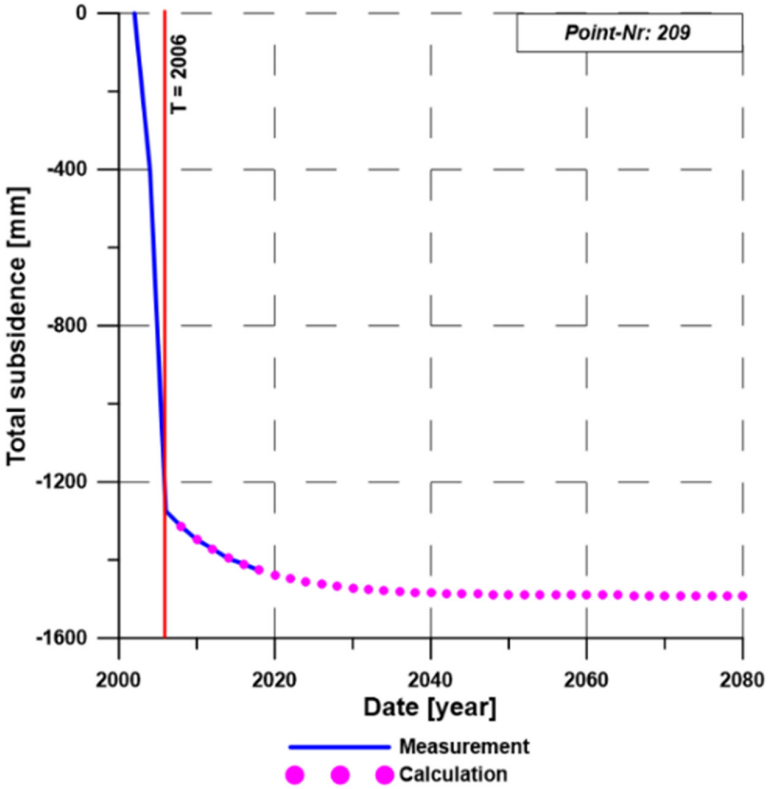

Figure 9. The course of subsidence until 2018 and the prediction of residual subsidence for the point no. 209.

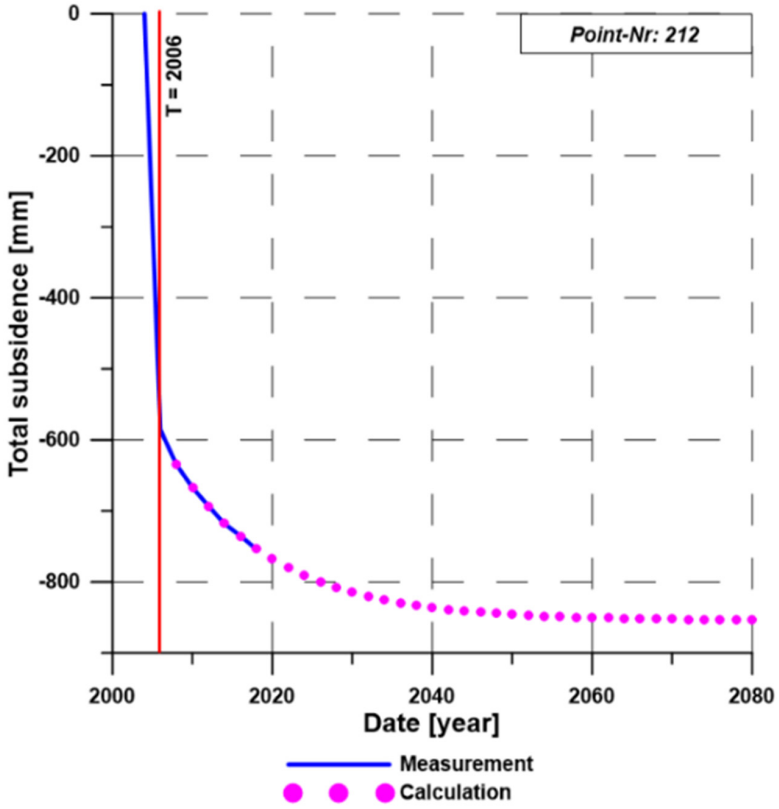

Figure 10. The course of subsidence until 2018 and the prediction of residual subsidence for the point no. 212.

4. Discussion

The problem of determining future land surface subsidence over the completed mining operation has so far been the subject of few scientific works. One of the most interesting approaches was the solution based on the so-called four- or three-point method. This approach, developed in the 1980s by Bartosik-Sroka [31], allows, on the absolutely basis of periodic subsidence measurements, for the determination of the future subsidence of the land surface with knowledge of the first observation of point subsidence after the end of mining operations. According to the solution, the course of subsidence is described by Formula (11). The method assumed the availability of an appropriate number of periodic observations of subsidence after the end of mining operations. Based on them, it was possible to make an approximate assessment of the value of the time coefficient c and the final subsidence of the analyzed point. The mathematical assumptions of the method are presented below.

With an appropriate number of measurements after the end of the mining operation, it is possible to evaluate the common function of time. Transforming Equation (11) obtained for the *ith* observation, one obtains:

$$\begin{aligned} &\frac{s(t_i)-s(t_1)}{s_e-s(t_1)} = \frac{\Delta s\left(\Delta t_{i,1}\right)}{\Delta s_{e,1}} = 1-\exp(-c\Delta t_{i,1}) \\ &\text{that is :} \\ &y(\Delta t_{i,1}) = 1-\exp\left(-x\left(\Delta t_{i,j}\right)\right) \end{aligned} \tag{21}$$

where:

$$x\left(\Delta t_{i,j}\right) = c\Delta t_{i,1}$$

The effectiveness of the application of the above mathematical solution based on the three-point and four-point methods was confirmed in the prognostic analyses of residual land subsidence conducted for the closed areas of several German underground coal mines [30].

On the other hand, the solution presented in the article, based on the Gauss–Markov algorithm, constitutes a new, innovative approach to the presented issue. As part of the research work, it was decided to compare the obtained results of land surface subsidence forecasts for both methods used. For this purpose, calculations were made for the sample measuring point No. 121. The obtained results were compared with those from the calculations using the three-point method (subsequent observations from 2008, 2012, and 2016 were selected for the analysis). Then, based on the formulas presented in Table 4, the values of the time coefficient and the final subsidence at the analyzed point were determined (for the three-point method):

$$c = 0.1175\ \left[\text{year}^{-1}\right],\ \ s_e = 816.70\ [\text{mm}]$$

$$s_c = \mp 0.0136\ \left[\text{year}^{-1}\right]$$

Table 4. Formulas of the three- and four-point method for estimating residual subsidence [31].

The Three-Point Method	The Four-Point Method
Final subsidence: $s_e = \frac{s_2^2 - s_3 s_1}{2s_2 - (s_3 + s_1)}$ Time coefficient: $c = -\frac{1}{\Delta t} ln \frac{s_3 - s_2}{s_2 - s_1}$ where: s_e—the final subsidence; s_i—the value of the point subsidence in time; Δt—the time interval between the observation.	Final subsidence: $s_e = \frac{s_3 s_2 - s_4 s_1}{(s_3 + s_2) - (s_4 + s_1)}$ Time coefficient: $c = -\frac{1}{\Delta t} ln \frac{s_4 - s_2}{s_3 - s_1}$

Comparing these values to the values obtained for the Gauss–Markov algorithm (from Table 2), it can be seen that the value of the time coefficient is almost twice as high, with a reduction in the final subsidence value by 3.0%.

Subsequently, based on the specified values of the time coefficient and the final subsidence for both methods, the subsequent point subsidence was calculated in time after the end of mining operations. Table 5 presents the results of the land surface measurements at the analyzed measurement points and the results of the calculations using the three-point method and the Gauss–Markov algorithm. Based on Table 5, it can be concluded that the Gauss–Markov algorithm allows for obtaining a better adjustment of the calculation curve to the measurement trough. This is because this method uses all recorded point measurements for the calculation. On the other hand, the three-point method for fitting the trough curve uses only three measurements (in the analyzed point 121, these are successive measurements in 2006, 2012, 2018). This is also confirmed in Figure 11.

Table 5. Results of the subsidence obtained using the three-point method s_{calc}^{3point} and Gauss–Markov s_{calc}^{G-M} equalization algorithm for point 121.

Year	s_{meas} [mm]	s_{calc}^{3point} [mm]	Δs [mm]	s_{calc}^{G-M} [mm]	Δs [mm]
2008	774.00	774.00	0.00	773.66	−0.34
2010	781.00	782.94	−1.94	782.06	1.06
2012	790.00	790.00	0.00	789.41	−0.59
2014	797.00	795.58	1.42	795.85	−1.15
2016	800.00	800.00	0.00	801.49	1.49
2018	807.00	803.49	3.51	806.43	−0.57

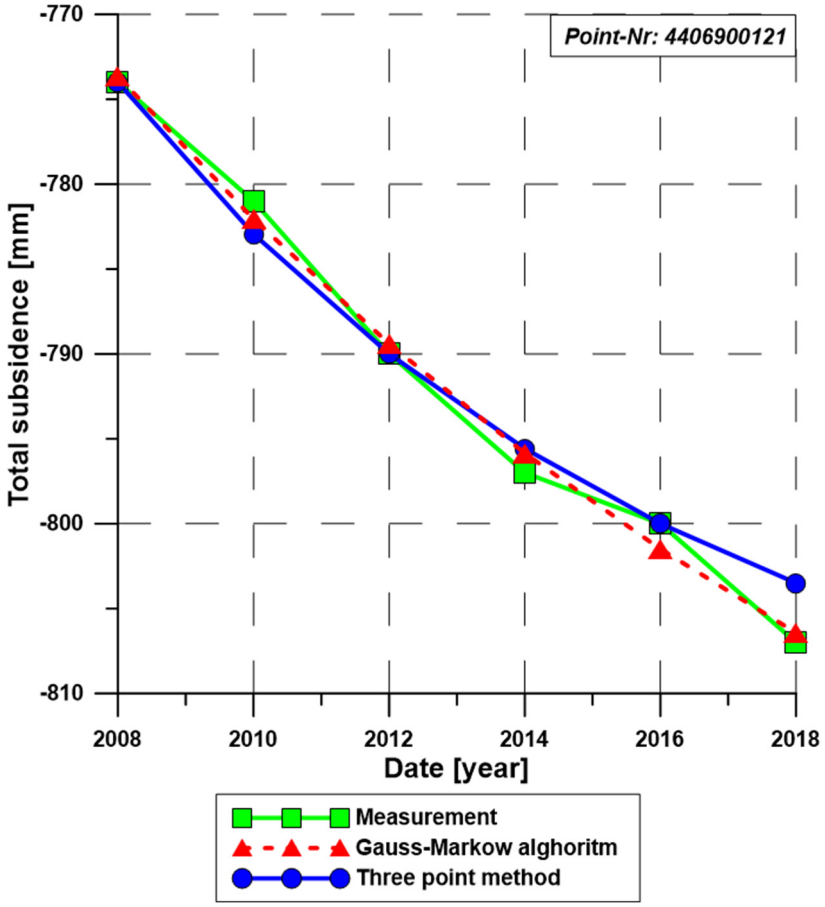

Figure 11. Comparison of the results of the three-point method and the Gauss–Markov algorithm for the point No. 121.

The above considerations clearly show that the use of the Gauss–Markov algorithm in conjunction with the functional model (here, the Knothe time function) gives a more accurate picture of reality. The model is able to react to measurement imperfections (e.g., the Figure 11 measurement in 2016). The three-point method, on the other hand, achieves such a match because the observations are adopted in the analysis, which may distort the prediction.

5. Conclusions

Exploitation causes a disruption of the initial balance of the rock mass. This leads to land surface deformation, changes in water relations, induced mining tremors, and, in some cases, mining damage. In terms of forecasting land surface deformation, this phenomenon has been studied for many years and many methods of forecasting this type of deformation have been developed. Most of them, however, refer to the condition of the land surface up to one year after the end of the mining operation. The article presents a solution with a methodology aimed at the best possible approximation of the duration and final value of deformation after the end of mining operations. Over time, an increasing amount of mines will be closed. Forecasting residual land surface deformation caused by mining is necessary to determine the measurement period and to assess potential future mining damage and the possibility of reusing the land degraded by mining activities. The presented calculation example for a mine belonging to the RAG concern (Lohberg) based on the proprietary solution and methodology using the Gauss–Markov algorithm shows that, in some cases, this time may last several or even several dozens of years.

Author Contributions: Conceptualization, A.S. and M.D.; methodology, A.S.; software, M.D.; validation, M.D., A.S. and M.D.; formal analysis, writing—original draft preparation, M.D.; writing—review and editing, A.S., K.T., M.D., D.M. and R.M.; visualization, M.D. and D.M.; supervision, A.S. and K.T. All authors have read and agreed to the published version of the manuscript.

Funding: This research received no external funding.

Data Availability Statement: Not applicable.

Acknowledgments: Part of the work in this paper was carried out as part of the statutory work of the Strata Mechanics Research Institute of Polish Academy of Sciences.

Conflicts of Interest: The authors declare no conflict of interest.

References

1. Krzemień, A.; Suárez Sánchez, A.; Riesgo Fernández, P.; Zimmermann, K.; González Coto, F. Towards sustainability in underground coal mine closure contexts: A methodology proposal for environmental risk management. *J. Clean. Prod.* **2016**, *139*, 1044–1056. [CrossRef]
2. Laurence, D. Optimisation of the mine closure process. *J. Clean. Prod.* **2006**, *14*, 285–298. [CrossRef]
3. Mishra, S.K.; Hitzhusen, F.J.; Sohngen, B.L.; Guldmann, J.-M. Costs of abandoned coal mine reclamation and associated recreation benefits in Ohio. *J. Environ. Manag.* **2012**, *100*, 52–58. [CrossRef] [PubMed]
4. Amirshenava, S.; Osanloo, M. Mine closure risk management: An integration of 3D risk model and MCDM techniques. *J. Clean. Prod.* **2018**, *184*, 389–401. [CrossRef]
5. Laurence, D. Classification of risk factors associated with mine closure. *Miner. Resour. Eng.* **2001**, *10*, 315–331. [CrossRef]
6. Dudek, M.; Tajduś, K.; Misa, R.; Sroka, A. Predicting of land surface uplift caused by the flooding of underground coal mines—A case study. *Int. J. Rock Mech. Min. Sci.* **2020**, *132*, 104377. [CrossRef]
7. Dudek, M.; Tajduś, K. FEM for prediction of surface deformations induced by flooding of steeply inclined mining seams. *Geomech. Energy Environ.* **2021**, *28*, 100254. [CrossRef]
8. Zhao, J.; Konietzky, H. Numerical analysis and prediction of ground surface movement induced by coal mining and subsequent groundwater flooding. *Int. J. Coal Geol.* **2020**, *229*, 103565. [CrossRef]
9. Zhao, J.; Konietzky, H. An overview on flooding induced uplift for abandoned coal mines. *Int. J. Rock Mech. Min. Sci.* **2021**, *148*, 104955. [CrossRef]
10. Chen, D.; Chen, H.; Zhang, W.; Cao, C.; Zhu, K.; Yuan, X.; Du, Y. Characteristics of the Residual Surface Deformation of Multiple Abandoned Mined-Out Areas Based on a Field Investigation and SBAS-InSAR: A Case Study in Jilin, China. *Remote Sens.* **2020**, *12*, 3752. [CrossRef]

11. Modeste, G.; Doubre, C.; Masson, F. Time evolution of mining-related residual subsidence monitored over a 24-year period using InSAR in southern Alsace, France. *Int. J. Appl. Earth Obs. Geoinf.* **2021**, *102*, 102392. [CrossRef]
12. Vervoort, A. The Time Duration of the Effects of Total Extraction Mining Methods on Surface Movement. *Energies* **2020**, *13*, 4107. [CrossRef]
13. Vervoort, A. Impact of the closure of a coal district on the environmental issue of long-term surface movements. *AIMS Geosci.* **2022**, *8*, 326–345. [CrossRef]
14. Cui, X.; Zhao, Y.; Wang, G.; Zhang, B.; Li, C. Calculation of Residual Surface Subsidence Above Abandoned Longwall Coal Mining. *Sustainability* **2020**, *12*, 1528. [CrossRef]
15. Knothe, S. Effect of time on formation of basin subsidence. *Arch. Min. Steel Ind.* **1953**, *1*, 1–7.
16. Sroka, A. Wpływ prędkości eksploatacji na deformacje powierzchni terenu. In Proceedings of the Szkoła Eksploatacji Podziemnej, Kraków, Poland, 22–26 February 2010; pp. 1–10.
17. Sroka, A.; Schober, F. Die Berechnung der maximalen Bodenbewegungen über kavernenartigen Hohlräumen unter Berücksichtigung der Hohlraumgeometrie. *Kali und Steinsalz* **1982**, *8*, 273–277.
18. Chen, Q.; Niu, W.; Liu, Y. Improvement of Knothe model and analysis on dynamic evolution law of strata movement in fill mining. *J. China Univ. Min. Technol.* **2017**, *46*, 250–256.
19. Chi, S.; Wang, L.; Yu, X.; Lv, W.; Fang, X. Research on dynamic prediction model of surface subsidence in mining areas with thick unconsolidated layers. *Energy Explor. Exploit.* **2021**, *39*, 927–943. [CrossRef]
20. Chang, Z.; Wang, J. Study on time function of surface subsidence—Improved Knothe time function. *Chin. J. Rock Mech. Eng.* **2003**, *22*, 1496–1499.
21. Deng, K.; Wang, J.Z.; Xing, A. On Predicting the Surface Subsidence Velocaty in Undermining Process. *J. China Univ. Min. Technol.* **1983**, *4*, 68–79.
22. Guo, X.W.; Yang, X.Q.; Chai, S.W. Optimization of the segmented Knothe function and its dynamic parameter calculation. *Rock Soil Mech.* **2020**, *41*, 2091–2097. [CrossRef]
23. Lian, X.; Jarosz, A.; Saavedra-Rosas, J.; Dai, H. Extending dynamic models of mining subsidence. *Trans. Nonferrous Met. Soc. China* **2011**, *21*, s536–s542. [CrossRef]
24. Knothe, S. Observations of surface movements under influence of mining and their theoretical interpretation. In Proceedings of the Proceeding European Congress on Ground Movement, Leeds, UK, 9–12 April 1957; pp. 210–218.
25. Hu, H.; Lian, X.; Li, Y.B. Application Study on the Dynamic Prediction Model for Determining the Mining Subsidence. *J. Eng. Sci. Technol. Rev.* **2016**, *9*, 80–85. [CrossRef]
26. Han, J.; Hu, C.; Zou, J. Time Function Model of Surface Subsidence Based on Inversion Analysis in Deep Soil Strata. *Math. Probl. Eng.* **2020**, *2020*, 4279401. [CrossRef]
27. Zhang, L.; Cheng, H.; Yao, Z.; Wang, X. Application of the Improved Knothe Time Function Model in the Prediction of Ground Mining Subsidence: A Case Study from Heze City, Shandong Province, China. *Appl. Sci.* **2020**, *10*, 3147. [CrossRef]
28. Cheng, H.; Zhang, L.; Guo, L.; Wang, X.; Peng, S. A New Dynamic Prediction Model for Underground Mining Subsidence Based on Inverse Function of Unstable Creep. *Adv. Civ. Eng.* **2021**, *2021*, 9922136. [CrossRef]
29. Niemeier, W. *Ausgleichungsrechnung: Eine Einführung für Studierende und Praktiker des Vermessungs-und Geoinformationswesens*; Walter de Gruyter: Berlin, Germany; New York, NY, USA, 2002.
30. Tajduś, K.; Sroka, A.; Misa, R.; Hager, S.; Rusek, J.; Dudek, M.; Wollnik, F. Analysis of Mining-Induced Delayed Surface Subsidence. *Minerals* **2021**, *11*, 1187. [CrossRef]
31. Bartosik-Sroka, T.; Pielok, J.; Sroka, A. Analitycal method of the time coefficient determination emloying results of periodical survay of the surface and strata subsidence. *Pr. Kom. Górniczo-Geodezyjnej. Geod.* **1981**, *29*, 51–62.